

## Polydirectional Stability of Granular Matter

Fabian Zimmer, Jonathan E. Kollmer, and Thorsten Pöschel

*Institute for Multiscale Simulation of Particulate Systems, Friedrich-Alexander-Universität Erlangen-Nürnberg,  
Naegelsbachstrasse 49b, 91052 Bavaria, Germany*

(Received 28 February 2013; published 18 October 2013)

We investigate jammed granular matter in a slowly rotating drum partially filled with granular material and find a state of polydirectional stability. In this state, the material responds elastically to small stresses in a wide angular interval while it responds by plastic deformation when subjected to small stresses outside this interval of directions. We describe the evolution of the granulate by means of a rate equation and find quantitative agreement with the experiment. The state of polydirectional stability complements the fragile state, where the material responds elastically to small applied stresses only in a certain direction but even very small stresses in any other direction would lead to plastic deformations. Similar to fragile matter, polydirectionally stable matter is created in a dynamic process by self-organization.

DOI: [10.1103/PhysRevLett.111.168003](https://doi.org/10.1103/PhysRevLett.111.168003)

PACS numbers: 45.70.-n, 81.05.Rm

In most situations, jammed granular matter responds elastically to small applied stresses irrespective of the direction of the applied forces. In some cases, however, the dynamics of granular flows may lead to states that respond elastically only to stress in certain directions. Even very small stress in any other direction would lead to plastic deformations. This fragile state has attracted much attention recently. The term fragile matter was coined by Cates *et al.* [1] as a state of granular matter that responds elastically only to compatible loads, in correspondence to its creation. If loaded incompatibly, that is, along a different direction, the packing responds plastically. The fragile state may be considered as a special case of jammed states; however, ordinary jammed matter may resist unidirectional stress (below the yield stress) while fragile matter undergoes plastic deformation even to small incompatible stress. In this sense, the fragile state extends the Liu-Nagel jamming diagram [2,3] in the limit of vanishing temperature. Since the pioneering work, Ref. [1], fragile systems have attracted much attention regarding both experimental [4–6] and theoretical or numerical [7–17] work.

Fragile states are generated from more dilute and mechanically unstable unjammed states, typically by application of shear [4]. As of now the necessary and sufficient conditions for material properties and dynamical processes leading to jamming into a fragile state are unknown.

In this Letter, by means of a rotating-drum experiment we show that besides the intensively discussed fragile state, there exists another, complementary state of jammed granular matter, which we call polydirectionally stable. In this state of rather low density, the material responds elastically to small stresses in a wide angular interval. The material is unstable against small stresses outside this angular interval—when loaded with small random stresses there is a constant probability of plastic response leading to sudden spatially located transformations to higher density, which we call collapse. This is similar to the fragile state

in that the system responds plastically or elastically depending on the direction of stress. It differs from the fragile state in that the angular range of elastic response is a wide interval whereas fragile matter responds elastically only against small stresses in a particular direction or a very narrow interval while all other stresses lead to plastic response. Similar to fragile states, polydirectionally stable states are the result of dynamical processes and depend on the system's history.

*Experimental setup.*—A cylinder of diameter 38 cm and width 0.4 cm rotates around its axis oriented perpendicular to gravity (see Fig. 1). The cylinder is half filled by about 400 g of sieved SiC granulate with grain size 125–150  $\mu\text{m}$ . These particles are sharply edged and optically sparkling, which allows for a convenient observation of particle motion. The cylinder consists of aluminium; the front and backplane are made from glass coated with ITO to avoid static charges. The experiment is recorded by a high-speed camera (500 fps, resolution  $1280 \times 1024$  pixels) and a camera at 1 fps. The cylinder rotates slowly at 1/7 revolutions per minute, chosen such that there is a narrow stripe of continuous flow at the free surface; neither avalanches nor stick-slip flow occur. All results presented are

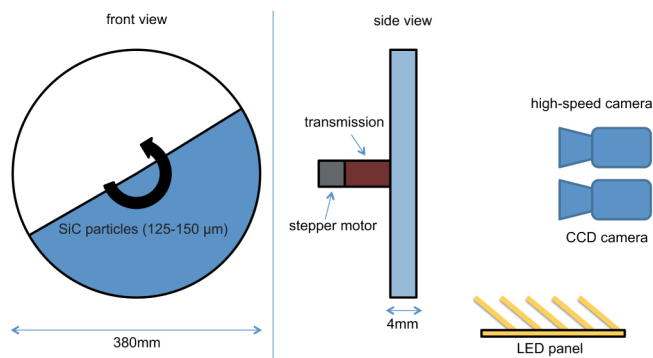


FIG. 1 (color online). Experimental setup.

insensitive to the rotation velocity as long as the flow is uniform (no stick-slip flow). Except for this narrow region the material rests with respect to the cylinder. That is, the material flowing along the free surface does not noticeably affect the bulk. Long intervals of this motion are interrupted by instantaneous consolidation events obeying a certain probability distribution where a large fraction of the system loses mechanical stability and collapses into a state of higher density.

There are numerous references, e.g., Refs. [18–22], on avalanches in rotating drums and inclines, regarding systems where catastrophic events occur at or close to the surface, in regimes where there is no continuous downhill flow. In contrast, the effect described here concerns large events in the bulk of the material that occur while the system is in continuous flow.

*Recurrent inflation and sudden collapse.*—Consider first the system’s long-time behavior. We apply connected component labeling to pictures taken in intervals of 1 sec, i.e.,  $0.86^\circ$  of rotation) to obtain the average space filling. We pour in the material (assume random close packing) and start the rotation at an approximately horizontal free surface. Initially,  $234 \text{ cm}^3$  out of  $454 \text{ cm}^3$  are occupied by particles ( $\eta = 0.51$ ).

After about two revolutions the system adopts its stationary state characterized by the angle  $\varphi_R \approx (38.1 \pm 0.1)^\circ$  between the free surface and the horizontal (counterclockwise rotation; we checked that the results are independent of the direction). As described below,  $\varphi_R$  changes abruptly by collapse events and recovers due to the rotation of the cylinder. Except for these short intervals of typical duration 2 sec,  $\varphi_R$  stays invariant during the entire experiment.

The stationary state is characterized by steady narrow downhill flow interrupted by sudden collapses of the sediment. During the flow regime the average space filling increases at constant rate by about 2% and shrinks due to collapse events by about the same amount.

Figure 2(a) shows the volume fraction over time for 1.65 h. Between collapses the volume increases linearly [see Fig. 2(b)]. Since we have constant rotation rate and

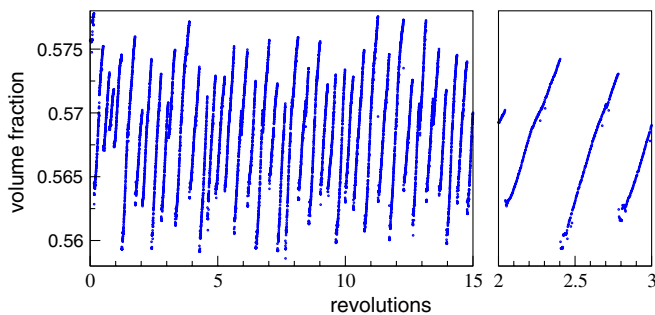


FIG. 2 (color online). (a) The volume fraction varies by  $\sim 2\%$  due to inflation in the steady flow regime and collapses. (b) Same data for shorter interval showing the inflation as a linear function of time. The error of the measurement is  $\pm 10^{-4}$ .

uniform flux due to constant inclination (except for a very short time just after the collapse) we conclude that the inflation results from the transfer of material of higher density  $\rho_c$  located at the right side of the cylinder into material of lower density  $\rho_d$  sedimented at the left side, where both  $\rho_d$  and  $\rho_c$  are homogeneous constants.

Comparing images immediately before and after a collapse we notice that the density of the material does not change uniformly. Figure 3(a) shows the image prior to the collapse overlaid by the image just after the collapse in reverse gray scale (the granulate and the background appear bright). Thus, the dark area identifies the region that vanished by the collapse, i.e., was lost because of transformation of loose material ( $\rho_d$ ) into material of higher density  $\rho_c$ . To estimate the ratio  $\rho_d/\rho_c$  we analyse the shape of the volume lost due to a collapse after a particularly long waiting time to assure that nearly all material in the cylinder is of low density  $\rho_d$ . The difference [see Fig. 3(b)] is approximately bound by the slopes  $\alpha_d \approx 38.0^\circ$  and  $\alpha_c \approx 36.5^\circ$ , and  $\Delta_H \approx 5.7 \text{ mm}$  is the height of the area. Note that we did not consider the area of the region to the right of the point where the surface touches the cylinder. We took this into account for the subsequent computation of  $\rho_d/\rho_c$ . The shape of the difference area together with the fact that the densities before and after the collapse are homogeneous constants leads to the conclusion that the region affected by the collapse has an approximately trapezoidal shape. To check this we measured the velocity field by means of particle image velocimetry

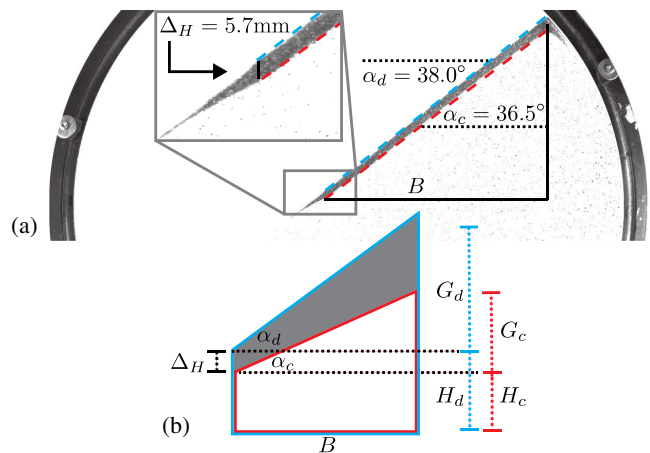


FIG. 3 (color online). (a) Overlay of images immediately before and after a collapse. The latter is drawn in reverse gray scale. Thus, the dark area was occupied by material before the collapse and is empty after it. Lines of slope  $\alpha_d$  and  $\alpha_c$  are fitted to the surface before and after the collapse. The magnification shows the difference region approximately bound by four straight lines, neglecting small transition regions at the very left and right. (b) Sketch of the trapezoidal difference region (gray shaded) and the region affected by the collapse, before (blue) and after (red) the collapse. The sketch also defines the quantities used for the analysis of the densification  $\rho_c/\rho_d$ .

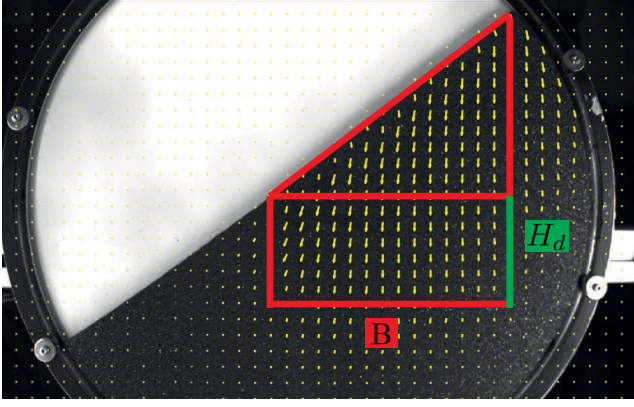


FIG. 4 (color online). Cumulative velocity field during a collapse. The region of nonvanishing velocity indicates the volume affected by the collapse. The trapezoid corresponds to the geometry introduced in Fig. 2. While  $B$  is clearly identified and  $G_d, H_c$  are known via  $\alpha_c$  and  $\alpha_d$  (see Fig. 3),  $H_d$  is less clearly determined. The height  $H_d$  was obtained from our model and agrees with the experiment; that is, below the marked area the arrows become negligibly small.

(PIV) using high speed recording of a collapse (see Fig. 4). The arrows show the cumulative velocity field summed over the duration of the collapse. The Supplemental Material [23] illustrates the process.

To check the hypothesis of an approximately trapezoidal shape we compare the difference volume [see Fig. 3(a)] with the putative collapsed volume, sketched in Fig. 3(b). Low-density material located in the triangle  $\triangle(B, G_d)$  collapses into  $\triangle(B, G_c)$ :

$$\rho_c B^2 \tan \alpha_c = \rho_d B^2 \tan \alpha_d. \quad (1)$$

With  $\alpha_c \approx 36.5^\circ$  and  $\alpha_d \approx 38.0^\circ$  obtained from Fig. 3(a), we find  $\rho_c/\rho_d = 1.056$ . Similarly, the material in the rectangle  $\square(B, H_d)$  collapses into  $\square(B, H_c)$ :

$$\rho_d B H_d = \rho_c B H_c = \rho_c B (H_d - \Delta H), \quad (2)$$

$$H_d = \frac{\Delta H}{1 - \frac{\rho_d}{\rho_c}}. \quad (3)$$

With  $\Delta H \approx 5.7$  mm from Fig. 3 we obtain  $H_d \approx 102.1$  mm which agrees well with PIV (see Fig. 4), supporting our hypothesis.

In all collapse events analysed by PIV the region of densification is restricted to the right-hand side of the cylinder, that is, loose material which is rotated by less than  $90^\circ - \varphi_R \approx 52.0^\circ$  was always found stable. Thus, after a collapse event, the region to the right of the cylinder's axis is in collapsed state  $\rho_c$ , while to the left of the axis the material is in the dilute state  $\rho_d$ . Therefore, for the following we found it reasonable to define  $\Theta$  with respect to the vertical line.

*Instability of packings.*—The distances between consecutive collapses are analyzed in Fig. 5.

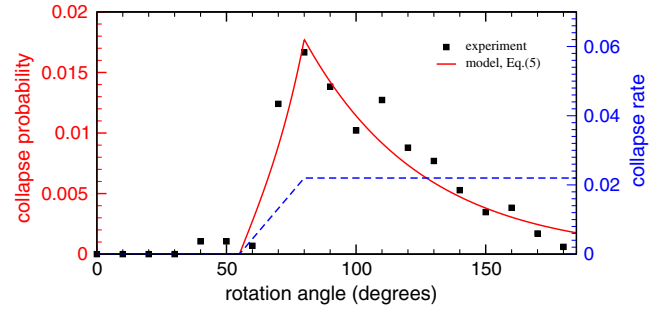


FIG. 5 (color online). Normalized frequencies of intervals between consecutive collapse events (points). Almost no collapses occur until the cylinder is rotated by about  $60^\circ$  after the preceding collapse. The solid line shows the probability density  $p(\Theta)$  [Eq. (5)] based on the rate model [Eq. (4)], sketched by the dashed line.

In the interval  $0^\circ \leq \Theta \leq 60^\circ$  after a collapse we find almost no collapses, followed by a peak at  $\Theta \approx 80^\circ$ . This means that the loose material  $\rho_d$  is stable (insensitive with respect to small perturbations) in the corresponding orientation.

We describe the probability density for the occurrence of a collapse by a rate model:

$$r_c(\Theta) = \begin{cases} 0 & \text{for } \Theta < \Theta_0 \\ r_0 \frac{\Theta - \Theta_0}{\Theta_1 - \Theta_0} & \text{for } \Theta_0 \leq \Theta \leq \Theta_1 \\ r_0 & \text{for } \Theta_1 \leq \Theta. \end{cases} \quad (4)$$

Assuming that for  $\Theta < \Theta_0$  the dilute material is stable and insensitive to small perturbations, which are always present when the cylinder is rotated. For  $\Theta > \Theta_1$  the material left its angular range of stability and even a small perturbation may cause a collapse. The interval  $(\Theta_0, \Theta_1)$  demarcates a small transition region where the material gradually loses stability. From  $r_c(\Theta)$ , we compute the probability density for the next collapse occurring at the angle  $\Theta$  after the preceding collapse:

$$p(\Theta) = \begin{cases} 0 & \text{for } \Theta < \Theta_0 \\ r_0 \exp\left(\frac{r_0}{2} \frac{(\Theta - \Theta_0)^2}{\Theta_1 - \Theta_0}\right) \frac{\Theta - \Theta_0}{\Theta_1 - \Theta_0} & \text{for } \Theta_0 \leq \Theta < \Theta_1 \\ r_0 \exp\left(\frac{r_0}{2} (3\Theta_1 - \Theta)\right) & \text{for } \Theta_1 \leq \Theta. \end{cases} \quad (5)$$

This distribution is shown in Fig. 5 with  $\Theta_0 = 60^\circ$  and  $\Theta_1 = 80^\circ$  taken from the experiment. The remaining free parameter  $r_0 = 0.022$  was determined by equating the expectation value  $\langle \Theta \rangle \equiv \int_0^\infty p(\Theta) \Theta d\Theta$ , according to Eq. (5), with the average angle of rotation between collapses  $\langle \Theta \rangle^{\text{exp}} \approx 108^\circ$  observed experimentally. Thus, without any fit parameters we obtain very good agreement between the distributions of the intervals between collapses seen in the experiment and the results of the model [Eq. (4)]. Figure 6(a) sketches the described angles and regions of stability.

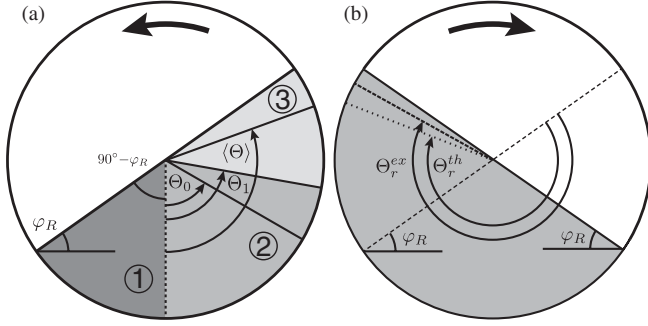


FIG. 6. (a) Counterclockwise rotation: definition of the angles  $\varphi_R$ ,  $\Theta_0$ ,  $\Theta_1$ ,  $\langle \Theta \rangle$ , and the regions of different type of stability: ①: always stable, low density,  $\rho_d$ ; ②: collapsed,  $\rho_c$ , or stable dilute,  $\rho_d$ ; ③: collapsed,  $\rho_c$ , or unstable dilute,  $\rho_d$ . (b) Clockwise rotation: definition of the angles  $\Theta_r^{ex}$  and  $\Theta_r^{th}$  (see text). The dashed line shows the surface of the material just before the reversal of rotation.

*Reversal of the rotation.*—To confirm our hypothesis on the wide angle of structural stability we reverted the sense of rotation as follows: we waited for a collapse-free interval of  $90^\circ + \varphi_R$  such that we can expect all material in the container in the dilute state. We then gently stopped the motion. The surface flow ceased immediately keeping its slope  $\varphi_R$  with respect to the horizontal. At this point ( $\Theta_r = 0$ ) we restarted the rotation in the opposite direction. The surface flow reemerged in the opposite direction at  $\Theta_r \approx -2\varphi_R \approx -76^\circ$  when the surface reached again the slope  $\varphi_R$ . Continuing the rotation, the first collapse was observed at  $\Theta_r \approx -225.7^\circ$  (average over ten repetitions); see Fig. 6(b) for a sketch of the process. Further continuing the rotation we found collapses in intervals  $\Delta\Theta_r$ , obeying the same statistics as reported before (see Fig. 5). This can be explained as follows: during the first interval  $\Theta_r = 0 \dots -2\varphi_R$  there is no surface flow, therefore, no random perturbations caused by flow at the free surface. Consequently, albeit the dilute material (once sedimented due to previous counterclockwise direction) is sensitive to random perturbations in this interval, we do not observe collapses. At this point,  $\Theta_r = -2\varphi_R$ , the material is already rotated back to an extent such that it is stable to small perturbations and we should not expect collapses of this material anymore. Continuing the rotation, for  $\Theta_r < -2\varphi_R$  dilute material from the left side of the cylinder moves down the slope and consolidates at the right. The sediment is also in the dilute state, but this time due to clockwise rotation. According to the arguments above for the counterclockwise motion, this material is stable for the next  $52^\circ$  ( $90^\circ - \varphi_R$ ), that is  $\Theta_r \in (-2\varphi_R, -90^\circ - \varphi_R)$ , until the dashed line in Fig. 6(b) turns vertical. From there, the expectation value for a collapse is  $-\langle \Theta \rangle \approx -108^\circ$  according to Eq. (5), where the minus sign comes from the reversed sense of rotation. Summing up, from our arguments and the expectation value of  $p(\Theta)$  [Eq. (5)] we predict  $\Theta_r = -90^\circ - \varphi_R - \langle \Theta \rangle \approx -236^\circ$  for the

next collapse. This result agrees with the experiment,  $\Theta_r = -225.7^\circ$ , up to 4.5% and, thus, supports our hypothesis that the material is stable against small forces in a wide range of angular orientation and turns unstable outside this interval.

*Conclusion.*—We investigated the structural stability of granular matter in a slowly rotating cylinder. In this regime, the material flows homogeneously (no avalanches nor stick-slip flow) in a small stripe down the slope keeping a time-invariant inclination. We found that the volume occupied by the material increases linearly in time, interrupted by sudden collapses where the volume reduces abruptly. Due to collapses the material densifies locally by  $\sim 5.3\%$ , whereas the other part of the volume is always unaffected. From the linear increase of the volume with time in between collapses and the steady flux down the slope we concluded that during the sedimentation process dense (previously collapsed) material of constant density  $\rho_c$  is transformed into material of constant lower density  $\rho_d$ . In the moment of consolidation, at the end of the downhill motion, the forces acting on the particles are determined in amplitude and direction by the angle of repose  $\varphi_R$  and gravity. According to the rotation of the entire cylinder the material, and thus each grain, turns and consequently feels static forces in directions different from the direction of the force at the moment of consolidation. This force is superimposed by small random forces caused by the small region of downhill flow at the free slope. Consequently, only material that rotated by more than a critical angle is affected by the collapse, which thus is always confined to the right side of the drum.

Based on experimental observations of the angular intervals between collapses, we set up a rate model [Eq. (4)] stating that the material is stable with respect to perturbations in the angular interval ( $0 \leq \Theta \leq \Theta_0$ ) and unstable for  $\Theta \geq \Theta_1$  with a small transition range ( $\Theta_0, \Theta_1$ ). The corresponding probability density  $p(\Theta)$  for the rotation  $\Delta\Theta$  between successive collapses agrees very well with the experiment.

Using the rate model, we identified three ranges of different type of stability: for  $\Theta \in (-90^\circ - \varphi_R, 0)$  [range ① in Fig. 6(a)] the material is always stable, for  $\Theta \in (0, \Theta_1)$  (range ②) it is stable against small perturbations but not against large perturbations, and for  $\Theta > \Theta_1$  it is unstable against perturbations (range ③). Thus, we find the sediment stable against small perturbations in the range  $\Theta \in (-90^\circ - \varphi_R, \Theta_1)$ , that is, a range of  $\sim 208^\circ$ .

The entire chain of arguments was verified for a different process taking place when we revert the sense of rotation.

Consequently, in this experiment we found a new state of dilute jammed granular matter that is stable against small perturbations in a wide angular interval of small stresses whereas it responds plastically when loaded with stresses outside this interval. This state of polydirectional stability thus complements the earlier found fragile state [1].

The necessary conditions for a system to adopt the state of polydirectional stability are not fully explored yet; however, clearly the particle shape plays an essential role: For smooth spheres, we do not observe the effect of recurrent inflation and collapse. The investigation of the influence of system and particle properties, and in particular of particle geometry, is the subject of current research.

We thank the German Science Foundation (DFG) for funding through the Cluster of Excellence 'Engineering of Advanced Materials'.

- 
- [1] M. E. Cates, J. P. Wittmer, J.-P. Bouchaud, and P. Claudin, *Phys. Rev. Lett.* **81**, 1841 (1998).
- [2] A. Liu and S. Nagel, *Nature (London)* **396**, 21 (1998).
- [3] A. Liu and S. Nagel, *Soft Matter* **6**, 2869 (2010).
- [4] D. Bi, J. Zhang, B. Chakraborty, and R. P. Behringer, *Nature (London)* **480**, 355 (2011).
- [5] A. I. Campbell and M. D. Haw, *Soft Matter* **6**, 4688 (2010).
- [6] B. Utter and R. P. Behringer, *Eur. Phys. J. E* **14**, 373 (2004).
- [7] M. E. Cates, J. P. Wittmer, J.-P. Bouchaud, and P. Claudin, *Physica (Amsterdam) A* **263**, 354 (1999).
- [8] M. E. Cates, J. P. Wittmer, J.-P. Bouchaud, and P. Claudin, *Chaos* **9**, 511 (1999).
- [9] R. Pastore, M. Pica Ciamarra, and A. Coniglio, *Granular Matter* **14**, 253 (2012).
- [10] K. Lu, E. E. Brodsky, and H. P. Kavehpour, *Nat. Phys.* **4**, 404 (2008).
- [11] C. Barbier, R. Dendievel, and D. Rodney, *Phys. Rev. E* **80**, 016115 (2009).
- [12] A. G. Smart and J. M. Ottino, *Phys. Rev. E* **77**, 041307 (2008).
- [13] M. Pica Ciamarra, R. Pastore, M. Nicodemi, and A. Coniglio, *Phys. Rev. E* **84**, 041308 (2011).
- [14] M. Sellitto and J. Kurchan, *Phys. Rev. Lett.* **95**, 236001 (2005).
- [15] F. Radjai and V. Richefeu, *Phil. Trans. R. Soc. A* **367**, 5123 (2009).
- [16] J.-N. Roux and G. Combe, *C.R. Phys.* **3**, 131 (2002).
- [17] S. R. Hostler and C. E. Brennen, *Phys. Rev. E* **72**, 031303 (2005).
- [18] R. Fischer, P. Gondret, and M. Rabaud, *Phys. Rev. Lett.* **103**, 128002 (2009).
- [19] N. Nerone, M. A. Aguirre, A. Calvo, D. Bideau, and I. Ippolito, *Phys. Rev. E* **67**, 011302 (2003).
- [20] S. Kiesgen de Richter, V. Y. Zaitsev, P. Richard, R. Delanny, G. Le Caër, and V. Tournat, *J. Stat. Mech.* (2010) P11023.
- [21] V. Y. Zaitsev, P. Richard, R. Delanny, V. Tournat, and V. E. Gusev, *Europhys. Lett.* **83**, 64003 (2008).
- [22] S. Deboeuf, O. Dauchot, L. Staron, A. Mangeney, and J.-P. Vilotte, *Phys. Rev. E* **72**, 051305 (2005).
- [23] See Supplemental Material <http://link.aps.org/supplemental/10.1103/PhysRevLett.111.168003> for a high speed recording of a collapse event, a video comparing the inflation-and-collapse regime to the regimes of surface avalanches and *s*-shape flow and a video demonstrating that collapse events do not occur in case of smooth spheres.